Tag-Compass: Determining the Spatial Direction of an Object with Small Dimensions

Jia Liu[†]   Min Chen[‡]   Shigang Chen[‡]   Qingfeng Pan[†]   Lijun Chen[†]

[†]State Key Laboratory for Novel Software Technology, Nanjing University, Nanjing 210023, China

[‡]Department of Computer & Information Science & Engineering, University of Florida, Gainesville, FL 32611, USA

Email: jialiu@nju.edu.cn   minchen@google.com   sgchen@cise.ufl.edu   chenlj@nju.edu.cn

Abstract—**Identifying an object's spatial direction (or orientation) plays a fundamental role in a variety of applications, such as automatic assembly, indoor navigation, and robot driving. In this paper, we design a fine-grained direction finding system called Tag-Compass that attaches a single tag to an object (whose size may be small) and identifies the tagged object's orientation by determining the spatial direction of the tag. We exploit the *polarization* properties of the RF waves used in the communications between an RFID reader and the tag on the object. Polarization mismatch between the tag and the reader's antenna affects the received signal strength at the reader. From the measured signal strength values, we are able to deduce the tag's direction through a series of transformations and deviation minimization. We propose a system design for Tag-Compass and implement a prototype. We evaluate the performance of Tag-Compass through extensive experiments using the prototype. The experimental results show that Tag-Compass provides accurate direction estimates with a median error of just $2.5°$ when the tag's position is known and a median error of $3.8°$ when the tag's position is unknown.**

I. Introduction

Radio-frequency identification (RFID) has wide applications in object tracking [1]–[3], supply chain management [4], [5], and warehouse inventory [6], [7]. The RFID tags are becoming ubiquitously available in our daily life as they make their way into retail products, library books, debit cards, passports, driver licenses, car plates, medical devices, etc. This paper studies an under-investigated problem, *identifying a tag's spatial direction*, which is of practical importance for a variety of applications. With the ability of determining a tag's direction, we will know the orientation of the object that the tag is attached to. In manufacturing, products on an assembly line may need to face towards a certain direction for automated operations such as painting, labeling, or component assembling [8], [9] to be performed at the correct area or spot on each product. It is thus useful as a quality control mechanism to automatically check the correct orientation of all or a randomly-sampled subset of tagged products on an assembly line right before the point of operation. If accurate orientation measurement can be made, the small number of misaligned objects may be moved back to face the correct direction by a robotic arm or other mechanisms. In a packaging company, the ability of detecting the exact orientation of tagged objects inside each package can help provide assurance at the end of a packaging line that objects are placed correctly inside (instead of upside down, for example). In indoor navigation systems, knowing the orientation of a tagged object can ensure reliable docking guidance towards the target of interest [10], [11].

In robotics, estimating the position and direction of a tagged robot offers critical information for autonomous driving [12].

Although much advancement was achieved on RFID-based applications in recent years, the problem of identifying an object's orientation has not received adequate attention. The most related work is RF-Compass [13], which is tailored to a specific application setting of robotic assembly, where a robot with several attached tags moves towards an object (e.g., a desk leg for assembly) which carries two tags. By comparing the signals from all tags, an RFID reader can roughly determine the positions of the two tags on the object through a space partitioning technique. The line segment between the two positions gives a reference about the object's orientation, based on which the robot will adjust its movement. The performance of RF-Compass relies on the localization accuracy of the two tags on the object, as well as the distance between the tags. For the general problem of identifying the orientation of an object, we may remove the robot from the system and replace its coarse localization function with the most advanced localization algorithms for RFID tags, such as PinIt [2] and DAH [3]. Both of them achieve great indoor localization accuracies, with the former having a median error of 11.2cm and the latter having a median error of 12.3cm. Such accuracies would be sufficient if the tagged object is long and thus the two tags can be far apart (for example, a couple of meters apart). However, if the object is short in the dimension(s) where the tags must be placed for measuring the direction, those best localization algorithms to update will be inadequate. For example, if the dimensions of the object in the horizontal plane (where the direction will be measured) are $20cm \times 20cm$, in our experiments, they result in mean directional errors of $30.0°$ and $31.6°$, respectively, which are too large for many applications.

This paper introduces Tag-Compass, a fine-grained direction finding system that uses a single tag to identify the orientation of the associated object; the single-tag solution can be applied to objects big or small, down to the size of the tag. Since even the state-of-the-art localization algorithms are proven to be inadequate, we resort to a completely different method based on the polarization properties of the RF waves used in the communications between an RFID reader and the tag on the object. The observation is that, as the RF waves travel from the reader to the tag and back, if the tag's direction and the polarization of the incoming wave (which is in turn determined by the reader antenna's direction) are not fully aligned, it causes *polarization mismatch*, thereby affecting the

received signal strength (RSS) at the reader. This power loss due to polarization mismatch is referred to as polarization loss factor (PLF). With the RSS values measured by the reader, we can derive PLF and further deduce the tag's relative direction with respect to the reader antenna's direction. With the latter a known quantity, we can then figure out the tag's absolute direction in space, which in turn gives us the object's orientation (whose relationship with the tag's direction is fixed after the tag is attached to the object). However, designing such a system is not simple because the received signal power relies on various physical-layer characteristics besides PLF, such as antenna gains, radiation pattern and reflection coefficients, whose values are unknown and may vary with environmental conditions.

In this paper, we propose a system design for Tag-Compass and a computational method that separates PLF from all other physical-layer characteristics (which will then be estimated as a whole). This allows us to isolate the impact of PLF, from which we can eventually determine the tag's direction. Tag-Compass is designed to operate under two cases, with the knowledge of the tag's position or without, which have their respective applications: in the previously-discussed assembly line application, the position where each product pauses for orientation measurement is fixed and known; in the indoor navigation case, the tag's position is not pre-known. Without knowing the tag's position a priori, we exploit two metrics, RSS deviation and angle variance, to build a family of holograms, which help us localize the tag. Even though our system also needs to figure out the tag's location, we use polarization properties as our main approach for direction finding. This new approach can tolerate localization error much better than the previous non-polarization approach that simply uses two tags' locations to determine a direction. Our experiments show that Tag-Compass has a median error of just $2.5°$ when the tag's position is pre-known and a median error of $3.8°$ when the tag's position is not known.

The main contributions of this paper are summarized as follows: First, this work performs fine-grained direction finding based on polarization properties and using a single tag. Second, its accuracy is far better than the prior art for objects of small dimensions. Third, we propose a novel RFID localization approach using RSS measurements. Fourth, we implement a prototype of Tag-Compass based on the commercial off-the-shelf (COTS) tags and readers, and demonstrate its performance through extensive experiments.

II. MOTIVATION AND BACKGROUND

A. Polarization and Object's Orientation

Polarized waves are electromagnetic waves in which the vibrations occur in a single plane. We use the term *polarization* for the direction of the electric field of a polarized wave, which is perpendicular to the propagation direction of the wave [14]. When the polarization direction is along a single line, the wave is linearly polarized. This paper uses linearly polarized waves in the communications between an RFID reader and a tag.

Most commercial tags (e.g., ALN-9640 Squiggle [15]) contain a narrow wire-like metal foil behaving like a dipole antenna: If the tag is fully aligned with the electric field of

incoming wave, the electrons are pushed back and forth from one end of the tag antenna to the other, ensuring sufficient voltage to power the integrated circuit for computation and communication. In contrast, if the tag is directed perpendicular to the electric field, electrons move back and forth just across the tiny width of the metal foil, producing no detectable voltage and thereby failing to drive the tag. For other angles between the tag and the electric field, the power level produced lies between the above two cases. The closer the angle is towards full alignment, the stronger the power that the tag produces, which is measurable by the reader from the reflected signal that it receives back from the tag.

This paper attempts to exploit the orientation-dependent physical characteristics of tag-reader communications for the purpose of identifying an object's orientation. We define the *direction of a tag* to be the direction from one end of the dipole to the other end; the starting end may be chosen arbitrarily. The *orientation of an object* can be conveniently defined under different application contexts. For a product on an assembly line, we may simply use the direction of its tag as its orientation. For a robot, we may define its orientation to be the direction which its face is pointing to. In general, after a tag is fixed onto an object, its direction of placement relative to the object's orientation is fixed. Hence, at any time, if we can figure out the absolute direction of the tag in space, we will know the orientation of the object. So the problem becomes determining the tag's direction. Next, we know the polarization of the incoming wave based on the direction of the reader's antenna, a quantity that can be controlled. Our conjecture is that there should be a way by which we can find the tag's absolute direction in space based on the strength of the reflected signal received by the reader from the tag, because we know that this signal strength is functionally related to the alignment between the direction of the tag and the polarization of the incoming wave (the latter is known).

B. Friis Equation

The extended Friis equation [16] provides a mathematical description of the power received by the receiver from the transmitter, as shown below.

$$P_R = P_T \frac{G_T G_R \lambda^2}{(4\pi r)^2}(1 - |\Gamma_T|^2)(1 - |\Gamma_R|^2)|\hat{\mathcal{P}}_T \cdot \hat{\mathcal{P}}_R|^2, \quad (1)$$

where P_R is the received power, P_T is the transmit power, λ is the wavelength, r is the distance between the transmitter and the receiver, G_R and G_T denote the angular-dependent receiver gain and transmitter gain, respectively, Γ_T indicates the transmitter reflection coefficient, Γ_R indicates the receiver reflection coefficient. Of most interest to us are $\hat{\mathcal{P}}_T$ and $\hat{\mathcal{P}}_R$, which are the *transmitter polarization vector* and the *receiver polarization vector*, specifying the polarization of the electromagnetic wave from the transmitter and the direction of the receiver's antenna in space, respectively. The squared dot product $|\hat{\mathcal{P}}_T \cdot \hat{\mathcal{P}}_R|^2$ of these two vectors is defined as the polarization loss factor (PLF).

The extended Friis equation describes the received power one way from the transmitter to the receiver. The communication between an RFID reader and a tag is a round trip, including the *uplink* from the reader to the tag, and the

downlink by which the tag backscatters the incoming wave back to the reader [14]. Therefore, derived from (1), the received power $P_{RX,reader}$ at the reader is given as following:

$$\begin{cases} P_{RX,reader} = P_{TX,reader} \times C^2 \times PLF \\ PLF = PLF{\uparrow} \times PLF{\downarrow} \\ C = \frac{G_{reader} \times G_{tag} \times \lambda^2}{(4\pi r)^2}(1 - |\Gamma_{reader}|^2)(1 - |\Gamma_{tag}|^2), \end{cases} \quad (2)$$

where $P_{TX,reader}$ is the original transmit power from the reader, C is called the *diversity* term capturing most parameters in (1) under notations in the context of reader-tag communication, $PLF{\uparrow}$ is the polarization loss factor of the uplink, $PLF{\downarrow}$ is the polarization loss factor of the downlink, and PLF is the product of the two. Most COTS readers, e.g., ALN-9900+ [17] and ImpinJ R420 [18], are able to measure the received power when a tag is successfully interrogated. The power is reported in a logarithmic form, referred to as RSS (Received Signal Strength), as follows.

$$\begin{aligned} RSS &= 10 \times \lg(P_{RX,reader}) \\ &= 10 \times (\lg P_{TX,reader} + 2\lg C + \lg PLF). \end{aligned} \quad (3)$$

With the RSS measurements by the reader, we develop Tag-Compass, which determines the tag's direction based on the polarization characteristics in tag-reader communications.

III. TAG-COMPASS OVERVIEW

A. System Deployment

Tag-Compass uses any widely-available commercial dipole tag, e.g., ALN-9640 Squiggle [15], as the vehicle to determine an object's orientation. As shown in Fig. 1(a), a dipole tag residing in the horizontal x-y plane is deployed on the top of an object. The vector connecting the two endpoints of the tag from A to B is the tag's direction, denoted by $\overrightarrow{AB}$. As shown in Fig. 1(b), we refer to the direction angle from the y-axis to $\overrightarrow{AB}$ as the *tag's direction angle*, denoted by β, $0 \leq \beta < 2\pi$, which also specifies the direction of the tag. Clearly, the tag's direction angle β will change by the same degrees (radians) as the tagged object changes its orientation. With a fixed angular relationship between the tag and the object, we can easily deduce the object's orientation from β.

Suppose the surveillance region is covered by one or a small number M of linearly polarized patch antennas (such as Larid PA9-12 [19]), denoted as $\mathcal{A} = \{A_1, A_2, ..., A_M\}$, with known locations, where $M \geq 1$. These antennas above the region hang from the ceiling and are parallel to the horizontal plane, as shown in Fig. 1(a). They are connected to a reader. For simplicity, we use A_m to represent the mth antenna as well as its coordinates, where $1 \leq m \leq M$. Each antenna A_m is able to electronically or mechanically rotate its polarization direction, i.e., the polarization of the generated waves. We refer to the incline angle between the y-axis and the polarization direction as *polarization angle*, denoted by θ, as shown in Fig. 1(b). Initially, the polarization is aligned with the y-axis, i.e., $\theta = 0$. When the polarization direction is rotated in cycles from $\theta = 0$ to $\theta = 2\pi$, the reader continuously schedules the antennas in round robin and collects the RSS sample measurements from the tag. For each antenna, we select a certain number N of samples, each
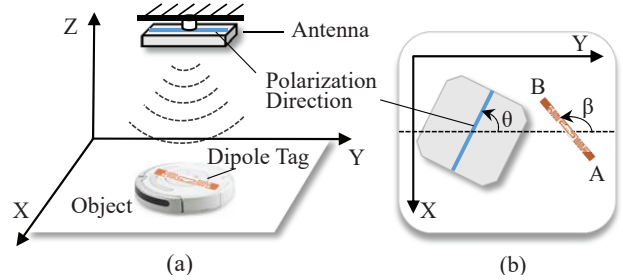

Fig. 1: (a) System deployment of Tag-Compass, (b) top view of antenna's polarization angle θ and tag's direction angle β.

having an RSS value and a value of θ at which the RSS measurement is taken. For example, in our experiments, we use $N = 18$ samples taken at polarization angles spaced between 0 and π about evenly.

Formally, we use a matrix $\mathcal{R}$ to depict the RSS measurements from all antennas.

$$\mathcal{R} = \begin{pmatrix} r_{1,1} & \cdot & r_{1,N} \\ \cdot & \cdot & \cdot \\ r_{M,1} & \cdot & r_{M,N} \end{pmatrix}, \quad (4)$$

where $r_{m,n}$ is the nth RSS value measured by the mth antenna, $1 \leq m \leq M$, $1 \leq n \leq N$. We also collect the corresponding polarization angle θ when each RSS value is measured:

$$\Theta = \begin{pmatrix} \theta_{1,1} & \cdot & \theta_{1,N} \\ \cdot & \cdot & \cdot \\ \theta_{M,1} & \cdot & \theta_{M,N} \end{pmatrix}, \quad (5)$$

where $\theta_{m,n}$ is the polarization angle of the mth antenna when collecting the nth RSS value, i.e., $r_{m,n}$. We formulate the direction finding problem as follows:

Problem 1: Given $\mathcal{A}$, $\mathcal{R}$, and Θ, how to determine the tag's direction angle β?

B. Solution Overview

Tag-Compass is designed to determine the tag's direction angle β in the following two cases.

● First, we consider the direction-finding problem with the priori knowledge of the tag's position, denoted as T. Such positional information can be automatically estimated through one of the numerous existing tag localization protocols [1]–[3]. With this information, we will discuss how to use $\mathcal{A}$ and Θ to fit the measured $\mathcal{R}$ and then derive β.

● Second, we remove the requirement of knowing the tag's position in advance. We propose three types of holograms to locate the tag first before determining the tag's direction angle.

IV. DIRECTION FINDING WITH KNOWN TAG POSITION

A. Rationale

The extended Friis equation (2) describes the received power by the reader. Consider an arbitrary reader's antenna A_m. From (2), when we rotate the polarization direction, all parameters except for the polarization loss factor stay unchanged. Therefore, the received power $P_{RX,reader}$ changes only with PLF as the polarization direction rotates. Given the measured RSS value (i.e., $P_{RX,reader}$), Tag-Compass will search the direction angle space to find the best angle whose PLF predicts a received power from (2) that matches best with the measured value.

B. Calculating PLF

Recall that the PLF in the round-trip RFID communication consists of $PLF\uparrow$ and $PLF\downarrow$. Consider an arbitrary reader antenna A_m. Denote its coordinates as (a_x, a_y, a_z). Let the tag's coordinates T be (t_x, t_y, t_z). The vector that specifies the tag's direction can be written as follows:

$$t(\beta) = (-sin\beta, cos\beta, 0), \tag{6}$$

where β is the tag's direction angle. For the uplink (from the antenna to the tag), the electromagnetic wave emitted by A_m travels along the vector $\overrightarrow{A_mT}$:

$$\overrightarrow{A_mT} = (i, j, k) = (t_x - a_x, t_y - a_y, t_z - a_z). \tag{7}$$

The polarization vector $u(A_m, T, \theta)$ of the electromagnetic wave at the tag's position T is:

$$u(A_m, T, \theta) = (u_1, u_2, u_3), \tag{8}$$

where θ is the polarization angle and

$$\begin{cases} u_1 = \frac{i \times (i \times sin\theta - j \times cos\theta)}{i^2 + j^2 + k^2} - sin\theta \\ u_2 = \frac{j \times (i \times sin\theta - j \times cos\theta)}{i^2 + j^2 + k^2} + cos\theta \\ u_3 = \frac{k \times (i \times sin\theta - j \times cos\theta)}{i^2 + j^2 + k^2}. \end{cases}$$

From (6) and (8), the polarization loss factor $PLF\uparrow$ of the uplink is:

$$PLF\uparrow(A_m, T, \theta, \beta) = |t(\beta) \cdot u(A_m, T, \theta)|^2. \tag{9}$$

Similarly, for the downlink, the polarization vector $d(A_m, T, \beta)$ of the electromagnetic wave (backscattered from the tag) at the point A_m is:

$$d(A_m, T, \beta) = (d_1, d_2, d_3), \tag{10}$$

where

$$\begin{cases} d_1 = \frac{i \times (i \times sin\beta - j \times cos\beta)}{i^2 + j^2 + k^2} - sin\beta \\ d_2 = \frac{j \times (i \times sin\beta - j \times cos\beta)}{i^2 + j^2 + k^2} + cos\beta \\ d_3 = \frac{k \times (i \times sin\beta - j \times cos\beta)}{i^2 + j^2 + k^2}. \end{cases}$$

Since the patch antenna, now as a receiver, can be treated as a horizontal panel, the polarization loss factor $PLF\downarrow$ of the downlink is equal to $cos^2\gamma$:

$$PLF\downarrow(A_m, T, \beta) = cos^2\gamma = \frac{d_1^2 + d_2^2}{d_1^2 + d_2^2 + d_3^2}, \tag{11}$$

where γ is the incident angle between $d(A_m, T, \beta)$ and the antenna panel, which remains stable regardless of the polarization angle θ. From (9) and (11), we obtain the PLF of the round-trip RFID communication:

$$PLF(A_m, T, \theta, \beta) = PLF\uparrow(A_m, T, \theta, \beta) \times PLF\downarrow(A_m, T, \beta). \tag{12}$$

With this mathematical description of PLF, we show how to estimate the tag's direction angle β below.

C. Estimating β

For each antenna A_m, we rotate its polarization direction and measure the RSS of the backscattered wave from the tag for N times, each time with a different polarization angle θ. We obtain two matrices for the measured values $\mathcal{R} = \{r_{m,n}\}$ and the corresponding angles $\Theta = \{\theta_{m,n}\}$, $1 \le m \le M$, $1 \le n \le N$, as defined previously in (4) and (5).

We want to determine the tag's direction angle β. To do so, we exhaustively search all possible angle values β' in the range of $[0, 2\pi)$ with a certain step size (e.g., $0.1°$). For any angle value β', we compute an RSS value $r'_{m,n}$, $\forall m \in [1, M], n \in [1, N]$, from (3) for each polarization angle $\theta_{m,n}$. We then find the angle value that minimizes the *deviation* (mean squared error) between the computed RSS values $r'_{m,n}$ and the measured values $r_{m,n}$. This angle value, denoted as $\hat{\beta}$, is our estimate for β. Hence, the formula for our estimation can be written as

$$\hat{\beta} = \underset{\beta' \in [0, 2\pi)}{argmin} \sum_{m=1}^{M} \sqrt{\sum_{n=1}^{N} (r'_{m,n} - r_{m,n})^2}. \tag{13}$$

Next we describe how to compute $r'_{m,n}$. From (3), we have

$$r'_{m,n} = 10 \times (\lg P_{TX,reader} + 2\lg C + \lg PLF). \tag{14}$$

The value of PLF can be computed from (12). But the value of C depends on many physical parameters of the antenna and the tag, whose precise values are difficult to determine for the following reasons: The values of some physical parameters such as reflection coefficients and antenna gains are often simply not available. One reason is that hardware characteristics may differ amongst individual tags, and it is impractical to calibrate all tags individually. Moreover, even if such parameters are determined for a tag before shipment, their values are typically measured in the anechoic chamber (equivalent to the free space), which may vary significantly from the actual operating environment.

Instead of dealing with the impact of physical parameters individually, we estimate all of them other than PLF as whole. Let $k_m = 10 \times (\lg P_{TX,reader} + 2\lg C)$. Replacing $r'_{m,n}$ with the measured value $r_{m,n}$ in (14), we have

$$k_m = r_{m,n} - 10 \times \lg PLF. \tag{15}$$

Taking the average over $1 \le n \le N$, we have the following estimate, denoted as $\hat{k_m}$:

$$\hat{k_m} = \frac{\sum_{n=1}^{N} (r_{m,n} - 10 \times \lg PLF)}{N}. \tag{16}$$

Replacing k_m with $\hat{k_m}$ in (15), we have

$$r'_{m,n} = \hat{k_m} + 10 \times \lg PLF, \ 1 \le n \le N. \tag{17}$$

We performed extensive experiments with the above formula in the process of determining the tag's direction angle. We use one example to demonstrate its excellent performance while most experimental results will be presented later. In this experiment, the true value of the tag's direction angle is $\beta = 50°$. With 18 RSS values measured from each antenna after every $10°$ of polarization rotation, we search through the β' values in $[0, 2\pi)$ with a step size of $0.1°$, and find the optimal estimate $\hat{\beta}$ based on (13) and (17). Fig. 2 shows the deviation between the computed RSS and the measured RSS with respect to the value of β'. As shown in Fig. 2(a) where one antenna is deployed, the deviation is minimized at $\beta' = 45.8°$. In this case, $\hat{\beta} = 45.8°$, which is very close to the true value of $50°$. Fig. 2(b) presents the deviations when two reader antennas are deployed. Its estimate is $\hat{\beta} = 46.4°$. As the number of antennas further increases, the estimate will become even closer to the true value. When one (two) antenna
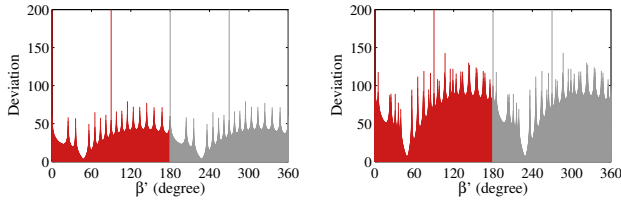
(a) One reader antenna   (b) Two reader antennas

Fig. 2: Deviation between the computed RSS and the measured RSS with respect to the value of β'.

(a) One reader antenna   (b) Two reader antennas

Fig. 3: Deviation between the computed RSS and the real RSS over the value of β' when the tag is inclined.

is used, the computation time of exhaustive search over the β' values is 4.5 ms (7.6 ms) on a Thinkpad T430s laptop with Intel i5-3210M CPU of 2.50GHz and 12GB memory.

D. Resolving Ambiguity

Tag-Compass however has an *ambiguity* issue, which may sometimes produce an estimate in the opposite direction. Take a closer look at Fig. 2. The deviation of β' actually presents a periodic pattern with period π (180°), i.e., the deviation of β' is about the same as that of $(\beta' + \pi)$, $0 \leq \beta' < \pi$. Hence, there are two possible estimates with about the same deviation during each execution of Tag-Compass, i.e., $\hat{\beta}$ and $\hat{\beta} + \pi$, $0 \leq \hat{\beta} < \pi$. The reason is due to a certain symmetry in placement: The tag is in a plane that is parallel to the plane of each antenna. In this case, if the tag is turned for 180°, the physical parameters in (2) for tag-antenna communication do not change. For some applications where the objects themselves are symmetric (such as a symmetric component on an assembly line), this ambiguity will not cause any problem because the objects can be used in either direction.

However, in other applications with asymmetric objects, we need to resolve the ambiguity. One way to break the ambiguity is to make the plane of the tag not parallel to the plane of the antenna. Let α be the incline angle between the tag direction and the x-y plane, which is preset during the tag deployment, without changing with β. Note that the tag's direction angle β is now from y-axis to $\overrightarrow{A'B'}$, where the points A' and B' are the projection of A and B on the x-y plane, respectively. When the tag rotates by π radians, the vector of the tag direction (including the direction and the numerical value) differs from the case of β. Formally, we have the vector of the tag direction:

$$\boldsymbol{t}(\beta, \alpha) = (-sin\beta cos\alpha, cos\beta cos\alpha, sin\alpha). \quad (18)$$

Accordingly, for the downlink, the polarization vector $\boldsymbol{d}(A_m, T, \beta, \alpha)$ of the electromagnetic wave reflected by the tag at the point A_m is:
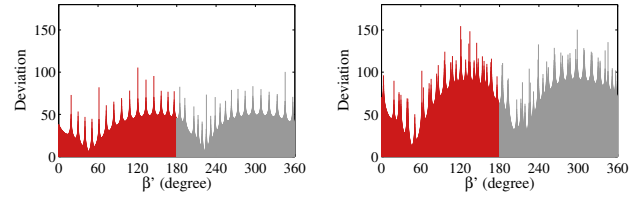
$$\boldsymbol{d}(A_m, T, \beta, \alpha) = (d'_1, d'_2, d'_3), \quad (19)$$

where

$$\begin{cases} d'_1 = \frac{i^2 sin\beta cos\alpha - ijcos\beta cos\alpha - iksin\alpha}{i^2+j^2+k^2} - sin\beta cos\alpha \\ d'_2 = \frac{ijsin\beta cos\alpha - j^2 cos\beta cos\alpha - jksin\alpha}{i^2+j^2+k^2} + cos\beta cos\alpha \\ d'_3 = \frac{(i^2+j^2)sin\alpha + ikcos\beta sin\alpha - jkcos\beta cos\alpha}{i^2+j^2+k^2}. \end{cases}$$

Similar to (12), the PLF of the round-trip communication is:

$$PLF(A_m, T, \theta, \beta, \alpha) = |\boldsymbol{u}(A_m, T, \theta) \cdot \boldsymbol{t}(\beta, \alpha)|^2 \frac{\sum_{i=1}^{2} d'^2_i}{\sum_{i=1}^{3} d'^2_i}. \quad (20)$$

The rest of the computation is the same as described previously. We repeat the experiment in Fig. 2 with the tag inclined by 30°, i.e., $\alpha = 30°$. The results are shown in Fig. 3. With a single antenna, the ambiguity is not satisfactorily resolved in Fig. 3(a). But when multiple antennas are deployed, the globally-minimum deviation achieved by $\hat{\beta}$ will be much smaller than other local minimums, effectively removing the ambiguity issue, as shown in Fig. 3(b).

V. DIRECTION FINDING WITHOUT PRE-KNOWN TAG POSITION

So far, we have discussed the system design of Tag-Compass under the case of knowing the tag's position (in the aforementioned assembly line application, for example). In other applications, such as indoor navigation, the tag's position may not be available at the time of direction finding. In this case, we may locate the tag first by using an existing RFID localization method [1]–[3], and then estimate the tag's direction angle. This design works but requires extra deployment for localization, which complicates our system. In this section, we perform localization and direction finding together based on the same measurement described in Section III-A, without introducing any extra deployment cost.

For ease of presentation, we present our approach in the 2D plane where the tag resides. The extension to the 3D space (in case that the tag may move vertically) is straightforward by adding one more dimension in searching for an estimated location of the tag that fits best with the observed data. We partition the surveillance area of interest into a grid of $L \times W$ squares at *cm* resolution. The centroid of each square is treated as a candidate position of the tag. The squares are denoted as $S_{l,w}$. We build three types of holograms: 1) RSS hologram, 2) Angle hologram, and 3) RSS-Angle hologram, in order to find the square at which the tag is located and then determine the tag's direction angle meanwhile.

A. RSS Hologram

The rationale of RSS Hologram (RH) is explained as follows: For each square $S_{l,w}$, $1 \leq l \leq L$, $1 \leq w \leq W$, we use its centroid as the tag position and obtain an estimate $\hat{\beta}_{l,w}$ value for the tag's direction angle from (13). Among these estimate values, we find the one with the smallest deviation between the computed RSS values and the measured RSS ones and use that value as the final estimated direction angle $\hat{\beta}$. And we use the centroid of the corresponding square as the estimated tag position. Based on the above idea, we build
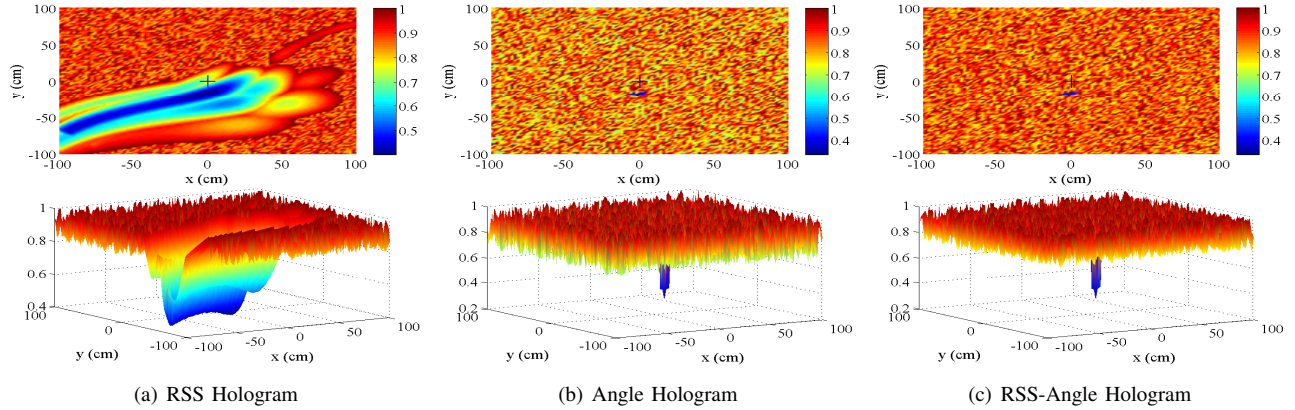
(a) RSS Hologram   (b) Angle Hologram   (c) RSS-Angle Hologram

Fig. 4: **Tag-Compass Holograms**. An image exhibition that depicts the likelihood of a square to be the tag position. The smaller the pixel value is, the more likely the square contains the tag. Three columns show RH/AH/RAH in 2D/3D images.

an RSS deviation-based image exhibition as follows.

$$
\text{RH} = \begin{pmatrix} h^r_{1,1} & \cdot & h^r_{1,W} \\ \cdot & \cdot & \cdot \\ h^r_{L,1} & \cdot & h^r_{L,W} \end{pmatrix} \tag{21}
$$

RH consists of $L \times W$ pixels. Each pixel $h^r_{l,w}$ is the minimal deviation between the measured RSS values and the computed RSS values assuming the tag is located in the square $S_{l,w}$. It is called *RSS deviation*:

$$
h^r_{l,w} = \min \sum_{m=1}^{M} \sqrt{\sum_{n=1}^{N}(r'_{m,n} - r_{m,n})^2}, \tag{22}
$$

where $r_{m,n}$ is the nth measured RSS value by the mth antenna and $r'_{m,n}$ is the corresponding computed value from (17). According to (13), the estimate angle $\hat{\beta}_{l,w}$ at square $S_{l,w}$ is:

$$
\hat{\beta}_{l,w} = \underset{\beta' \in [0,2\pi)}{\operatorname{argmin}} \sum_{m=1}^{M} \sqrt{\sum_{n=1}^{N}(r'_{m,n} - r_{m,n})^2}. \tag{23}
$$

Among the $L \times W$ squares, the one $S_{l,w}$ with the minimal pixel value $h^r_{l,w}$ is considered to contain the tag, and the corresponding $\hat{\beta}_{l,w}$ is used as the final estimate for the tag's direction angle. Formally, we have the estimate $\hat{\beta}$ as follows:

$$
\hat{\beta} = \hat{\beta}_{l,w}, \quad \text{where } [l, w] = \underset{1 \le l \le L; 1 \le w \le W}{\operatorname{argmin}} (h^r_{l,w}). \tag{24}
$$

We show the results of an experimental study with three linearly polarized antennas in Fig. 4, where the antennas cover a 2D plane of $200cm \times 200cm$. The tag is located at the origin $(0,0)$ with an incline angle of $30°$. The distance between the tag and the antenna plane is $1.5m$ and the true direction angle of the tag is $50°$. The step size of the direction angles and the edge length of each square are set to $0.5°$ and $2cm$, respectively. The RH is built according to (21), as shown in Fig. 4(a). Each pixel in this image is the normalized result and the blue colors denote small deviation values. The estimated tag position is $(-14, -18)cm$ and the corresponding direction angle is $56.8°$, which are close to the real values. Although RH achieves good localization and angle estimate, there is a large stretch of the blue area with small deviation values, which may sometimes degrade the accuracy in localization and angle estimate. Below we propose a more reliable method.

B. Angle Hologram

For each square $S_{l,w}$, $1 \le l \le L$, $1 \le w \le W$, we use its centroid as the tag position and then use the measured RSS values from each antenna to make a separate estimate for the tag's direction angle — there will be M estimates for M antennas. If $S_{l,w}$ contains the tag, all M estimates will be close to each other. Otherwise, the estimates will be different. This difference, captured by *angle variance* below, is dependent on how far the square is away from the true position of the tag. We build Angle Hologram (AH) below:

$$
\text{AH} = \begin{pmatrix} h^a_{1,1} & \cdot & h^a_{1,W} \\ \cdot & \cdot & \cdot \\ h^a_{L,1} & \cdot & h^a_{L,W} \end{pmatrix} \tag{25}
$$

where each pixel $h^a_{l,w}$ records the variance of the M estimates of the tag's direction angle computed based on the measurements from the M antennas, assuming the tag is located at the square $S_{l,w}$. This variance is called *angle variance*:

$$
h^a_{l,w} = \frac{1}{M} \sum_{m=1}^{M} (\hat{\beta}_{l,w}(A_m) - \mu_{l,w})^2, \tag{26}
$$

where

$$
\begin{cases} \mu_{l,w} = \frac{1}{M} \sum_{m=1}^{M} \hat{\beta}_{l,w}(A_m) \\ \hat{\beta}_{l,w}(A_m) = \underset{\beta' \in [0,2\pi)}{\operatorname{argmin}} \sum_{n=1}^{N}(r'_{m,n} - r_{m,n})^2. \end{cases} \tag{27}
$$

The term $\hat{\beta}_{l,w}(A_m)$ is the estimate of the direction angle based on the RSS measurements by the antenna A_m, and $\mu_{l,w}$ is the mean of the M estimates by the M antennas. If the square $S_{l,w}$ contains the tag position, the variance $h^a_{l,w}$ will be smaller than those of other squares. Hence, we use the square $S_{l,w}$ with the minimal $h^a_{l,w}$ value to estimate the tag's location. The final estimate $\hat{\beta}$ of the tag's direction angle is as follows.

$$
\hat{\beta} = \mu_{l,w}, \quad \text{where } [l, w] = \underset{1 \le l \le L; 1 \le w \le W}{\operatorname{argmin}} (h^a_{l,w}). \tag{28}
$$

However, there is the ambiguity issue when we use one antenna A_m to find the direction angle $\hat{\beta}_{l,w}(A_m)$; see Section IV-D. To solve this problem, we compute $\hat{\beta}_{l,w}$ via (23) first for each square $S_{l,w}$, which does not have the ambiguity issue because all M antennas are used. We then compute $\hat{\beta}_{l,w}(A_m)$; if ambiguity arises, we choose the value that is closer to $\hat{\beta}_{l,w}$. It may appear that AH will take much longer time than RH

to compute, but in reality that is not the case. Most of the computation for $\hat{\beta}_{l,w}(A_m)$, $1 \leq m \leq M$, can benefit from the intermediate results in computing $\hat{\beta}_{l,w}$. Hence, we find in our implementation that AH takes almost the same time as RH, with negligible difference.

Fig. 4(b) shows the AH under the same experimental setting as in Fig. 4(a). Clearly, only a small patch of blue zone is left with small deviation values, effectively excluding all squares that are not close to the tag at $(0,0)$. With AH, the estimated tag position is $(-8, -18)cm$ and the direction angle is $56.2°$.

C. RSS-Angle Hologram

RH and AH provide two metrics, RSS deviation and angle variance, for estimating the tag's position and direction angle. We take a further step to combine them for an RSS-Angle Hologram (RAH), as defined below.

$$\text{RAH} = \begin{pmatrix} h_{1,1} & . & h_{1,W} \\ . & . & . \\ h_{L,1} & . & h_{L,W} \end{pmatrix} \quad (29)$$

Each pixel $h_{l,w}$ is calculated as follows:

$$h_{l,w} = h_{l,w}^r \times h_{l,w}^a, \quad (30)$$

where $h_{l,w}^r$ and $h_{l,w}^a$ are calculated by (22) and (26), respectively. As previously mentioned, smaller $h_{l,w}^r$ and $h_{l,w}^a$ values indicate higher likelihood to contain the tag position. Hence, we use the square $S_{l,w}$ with the minimal $h_{l,w}$ value as an estimate for the tag's location:

$$[l, w] = \underset{1 \leq l \leq L; 1 \leq w \leq W}{\arg\min} (h_{l,w}). \quad (31)$$

After this square is determined, we estimate the direction angle in the following.

$$\hat{\beta} = \frac{1}{2}(\hat{\beta}_{l,w} + \mu_{l,w}), \quad (32)$$

where $\hat{\beta}_{l,w}$ and $\mu_{l,w}$ can be calculated by (23) and (27), respectively. Fig. 4(c) presents the RAH under the same experimental deployment as in Fig. 4(a) and Fig. 4(b). RAH not only keeps a small blue area as AH, but also widens the likelihood gap between blue area and other area. With RAH, the estimated tag position is $(-6, -16)cm$ and the estimated direction angle is $55.4°$, very close to the true values.

D. Hierarchical Search

We propose a hierarchical search method to reduce the computation time of the RH/AH/RAH methods. This might be important when the surveillance area is large or the tag moves in the 3D space. Fine-grained partition of the surveillance area produces accurate estimate results, but suffers from high computation overhead. To reduce the overhead, we adopt two-level hierarchical search that begins with a coarse-grained area partition in order to quickly locate a large square where the tag resides, and then partitions the large square into small squares and perform the search a second time for accurate estimation of tag location and direction angle. This search strategy can be generalized to more than two levels. Our experiment results show that the hierarchical search can dramatically speed up hologram building to less than half a second, at a small expense of accuracy loss.
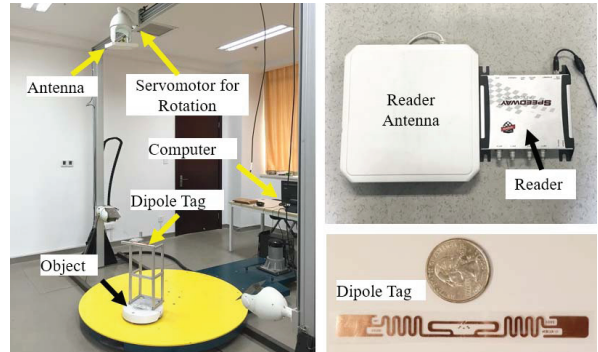

Fig. 5: Experiment setups.

VI. IMPLEMENTATION & EVALUATION

We have developed a prototype of Tag-Compass to evaluate the system performance, as shown in Fig. 5.

Reader: We use an Impinj Speedway R420 reader [18], which provides four RP-TNC ports to support four antenna connections at most. In our experiments with more than four antennas, we use an Antenna Hub [18] which allows a single reader to support up to 32 antennas. We stress that although we evaluate our system with the number of antennas going beyond four, we believe in practice one through four antennas will be sufficient, depending on the application requirements on ambiguity resolution and direction-estimation accuracy.

Antennas: We use the Larid PA9-12 patch antennas [19], which are direction-sensitive linearly polarized antennas. These antennas are hung from the holders on a gantry and uniformly scheduled by the reader in round robin [3]. Each holder is equipped with a servo motor that can rotate the antenna continuously. In practice, one may want to use the technique of dynamic polarization control (DPC) [20] to set the polarization of the far-field electric field generated by a radiating antenna in an electronically controlled manner, without any mechanical configuration. For example, by controlling the amplitude and the phase, Bowers et al. [20] designed a DPC-enabled antenna that is able to electronically change the polarization angle across the entire tuning range of $0°$ to $180°$.

Tags: On the top of an object, we attach a dipole ALN 9640 tag [15], which is sensitive to the polarization of the incoming waves. The tag is located in a surveillance plane of size $200cm \times 200cm$.

Based on the above deployment, we evaluate the performance of our system in two cases: 1) known tag position and 2) unknown tag position.

A. Evaluation with Tag Position

1) Accuracy: The most related work is RF-Compass [13] that uses iterative space partition to identify an object's orientation. As is explained in the introduction, RF-Compass involves two tags on the object and several tags on a robot that approaches towards the object. Essentially, it uses the tags on the robot to help locate the two tags on the object through the space-partitioning technique. Once the approximate locations of two tags on the object are known, the line segment between these locations provides a reference for the object's orientation. This will not work well if the objection's dimensions are small so that the tags are close to each other. RF-Compass
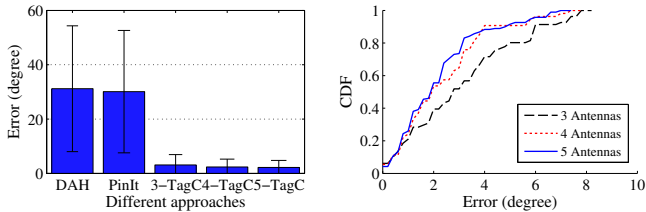
Fig. 6: Accuracy comparison. Fig. 7: Accuracy of Tag-Compass

Fig. 8: Impact of direction angle.Fig. 9: RAH-based Localization.

is designed for a specific robotic setting, whereas this paper studies the general problem of direction finding. Therefore, in order to make comparison in the context of this paper, we simplify and improve the performance of RF-Compass by removing the robot of several tags and instead using the more advanced tag-localization algorithms, PinIt [2] and DAH [3], which will give more accurate tag coordinates and thus give better estimate of the tag's direction. As we demonstrate below, except for large objects of sizes in meters, the start-of-the-art algorithms do not provide sufficient localization precision for direction finding.

Modified RF-Compass with PinIt: In the experiment, we let the two tags on the object be $20cm$ apart. PinIt [2] exploits a tag's multipath profile to locate it. The underlying rationale behind PinIt is that nearby tags experience a similar multipath environment and thus exhibit similar multipath profile. PinIt aims to estimate the tag position in a manner robust to multipath and non-line-of-sight, but it needs an antenna array (or a mobile antenna) and many references tags to cover the surveillance area. According to [2], PinIt achieves a median error of $11.2cm$ in localization, with a standard deviation of $6.2cm$. Applying it on direction finding, our experiment shows that it has a mean error of $30.0°$ with a standard deviation of $23.2°$, as shown in Fig. 6. We want to stress that this result does not at all mean that RF-Compass has a questionable design. On the contrary, it is a great design in its context where iterative adjustment of robot movement is used to compensate the inaccuracy in direction finding. However, in a more general non-robotic context with smaller objects, we need better tools for direction finding.

Modified RF-Compass with DAH: DAH [3] builds a differential augmented hologram using the phase values for localizing a tag. Compared with PinIt, DAH is more scalable in RFID applications as it does not need to pre-deploy reference tags for accurate calibration. It needs multiple antennas and requires the object (or the antennas) to be moving in order to locate the tag. In the case where the tag's trajectory is unknown, DAH has a median error of $12.3cm$ in localization, with a standard deviation of $5cm$. Applying it on direction finding, our experiment shows that DAH has a mean error of $31.6°$ with a standard deviation of $21.5°$, as shown in Fig. 6.

Tag-Compass: In Fig. 6, when three antennas are deployed, Tag-Compass has a median error of $3.1°$ in direction finding, with a standard deviation of $3.8°$; when four antennas are deployed, Tag-Compass has a median error of $2.5°$ in direction finding, with a standard deviation of $1.7°$, outperforming DAH and PinIt by 12.6 times and 12.0 times, respectively. Taking a closer look at the accuracy comparison, Fig. 7 plots the CDFs of the estimate error by Tag-Compass. With four antennas,
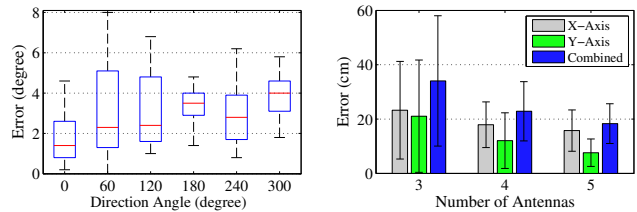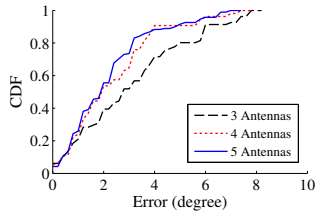
Tag-Compass's 90th percentile is $4.3°$, and 99th percentile is $7.0°$, achieving high precision within a few degrees. The estimation accuracy will be further improved as the number of antennas increases. This performance benefits from high sensitivity of dipole tags to polarization orientation.

2) Impact of Direction Angle: In Fig. 8, we study the estimate accuracy of Tag-Compass with respect to the direction angles. The tag inclines $30°$ and rotates from $0°$ to $360°$, with a step of $60°$. In each direction angle, we deploy four antennas to identify this tag's direction angle. As shown in this figure, the tightness (small errors) between the estimated value and the real value well indicates that Tag-Compass can achieve a high resolution of estimation under different direction angles.

B. Evaluation without Tag Position

In the following experiments, we relax the assumption of knowing the tag position in advance.

1) Localization Accuracy: Fig. 9 depicts the localization accuracy of RAH under different scenarios, where three, four, and five antennas are respectively deployed to cover a surveillance region with the size of $200cm \times 200cm$. The tag is located at the origin $(0, 0)$. For a given number of antennas, we conduct 50 groups of experiments to evaluate the localization accuracy in x-axis, y-axis, and the 2D plane (under the label "combined" in the figure). As shown in this figure, when three antennas (3-RAH) are used, our method RAH achieves a mean error of $21.2cm$, $23.4cm$, and $35.3cm$ in above dimensions, outperforming most RSS-based localization algorithms. With the increase of antennas, the localization accuracy of RAH increasingly improves in all three dimensions. For example, with five antennas (5-RAH), our approach achieves the localization with mean error of $15.4cm$, $8.5cm$, and $18.7cm$ in x-axis, y-axis, and 2D plane. This is a great improvement on the localization accuracy compared with 3-RAH, much close to the state-of-the-art PinIT [2] and DAH [3]. We assert that Tag-Compass provides a novel and accurate RSS-based localization technique, with no need of any reference tag deployment.

2) Accuracy of direction angle: In Fig. 10, we study the accuracy of RH, AH, and RAH in estimating the direction angle of the tag. When three antennas are deployed in Fig. 10(a), RAH performs best, RH and RA follow and perform equally well. With the increase of antennas, the estimation accuracy of RH, AH, and RAH improves significantly. For example, RAH with four antennas achieves a median error of $3.8°$, with the standard variance $3.6°$, as shown in Fig. 10(b). Note that RH is much worse than others as the number of antennas increases. That is because the holograms provide different localization results under different antenna deployment. These results are close to, but not exactly the same as, the real
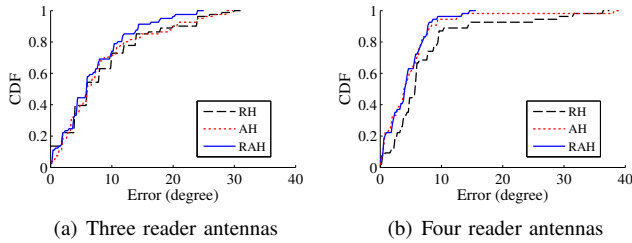
(a) Three reader antennas   (b) Four reader antennas

Fig. 10: Accuracy of angle estimation without tag position.

(a) Localization accuracy   (b) Angle accuracy

Fig. 11: Hierarchical search vs. fine-grained search.

tag position. It is hard for RH's angle estimate in a position to closely resemble that in another different position. By contrast, each antenna in AH individually searches the optimal angle which is randomly distributed around the ground truth. The mean of all estimated angles enables AH to decrease the variance, thereby performing better than RH. In conclusion, our proposed three holograms can achieve accurate direction finding with no priori knowledge of the tag position. This high performance also demonstrates that our estimate approach is able to tolerate the localization deviation to some degree.

3) Hierarchical Search: In this experiment, we investigate the performance gain as well as the accuracy loss of the hierarchical search, compared with that of the fine-grained one-level search. In the fine-grained search, the edge length of the squares is set to $2cm$ and the step size of the angle search is set to $0.5°$. In the two-level hierarchical search, we set the parameters as follows: At the first level, we set the edge length to $20cm$, and the step size of the angle to $1°$. After finding the square with minimum deviation, at the second level, we zoom in to this square and search the $20cm \times 20cm$ area using the same granularity as the fine-grained search. Under this setting, we compare the execution time of the both search methods: When four antennas are deployed, the hierarchical search takes only 0.34s to build RAH for localization and angle estimation, which obtains about $70\times$ performance gain compared with 23.2s of the fine-grained search. Besides, we check the accuracy loss of the hierarchical search. Fig. 11(a) depicts the localization accuracy of RAH under different number of antennas. As we can see, the fine-grained search only slightly outperforms the hierarchical search. The similar conclusion can also be drawn on the angle estimation, as shown in Fig. 11(b). To sum up, we say that the hierarchical search can greatly speed up the execution of Tag-Compass, at a very small expense of accuracy loss.

VII. Conclusion

In this paper, we propose Tag-Compass, a fine-grained direction finding system. The key innovation of Tag-Compass is to determine an object's orientation by estimating the direction of a single RFID tag based on the polarization properties of electromagnetic waves exchanged between the tag and a reader's antennas. We develop an insight into the relationship between the RSS values and the tag direction and apply this insight to estimate the latter through a series of transformations and deviation minimization, starting from the RSS values measured by the reader. Extensive experiments demonstrate that Tag-Compass can determine a tagged object's orientation with an error of only a few degrees.
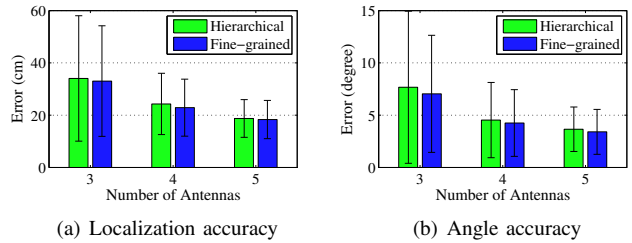
References

[1] L. Ni, Y. Liu, Y. C. Lau, and A. Patil, "LANDMARC: Indoor location sensing using active RFID," in *Proc. of IEEE PerCom*, 2003, pp. 407–415.

[2] J. Wang and D. Katabi, "Dude, where's my card?: RFID positioning that works with multipath and non-line of sight," in *Proc. of ACM SIGCOMM*, 2013, pp. 51–62.

[3] L. Yang, Y. Chen, X.-Y. Li, C. Xiao, M. Li, and Y. Liu, "Tagoram: Real-time tracking of mobile RFID tags to high precision using cots devices," in *Proc. of ACM MobiCom*, 2014, pp. 237–248.

[4] C.-H. Lee and C.-W. Chung, "RFID data processing in supply chain management using a path encoding scheme," *IEEE Trans. on Knowl. and Data Eng. (TKDE)*, vol. 23, no. 5, pp. 742–758, 2011.

[5] S. Qi, Y. Zheng, M. Li, Y. Liu, and J. Qiu, "Scalable data access control in RFID-enabled supply chain," in *Proc. of IEEE ICNP*, 2014, pp. 71–82.

[6] X. Liu, S. Zhang, B. Xiao, and K. Bu, "Flexible and time-efficient tag scanning with handheld readers," *IEEE Trans. on Mob. Comput. (TMC)*, vol. 15, no. 4, pp. 840–852, 2016.

[7] J. Liu, B. Xiao, S. Chen, F. Zhu, and L. Chen, "Fast RFID grouping protocols," in *Proc. of IEEE INFOCOM*, 2015, pp. 1948–1956.

[8] S. Jorg, J. Langwald, J. Stelter, G. Hirzinger, and C. Natale, "Flexible robot-assembly using a multi-sensory approach," in *Proc. of IEEE ICRA*, vol. 4, 2000, pp. 3687–3694.

[9] M. Bonert, L. H. Shu, and B. Benhabib, "Motion planning for multi-robot assembly systems," *International Journal of Computer Integrated Manufacturing*, vol. 13, no. 4, pp. 301–310, 2000.

[10] M. Kim and N. Y. Chong, "RFID-based mobile robot guidance to a stationary target," *Mechatronics*, vol. 17, no. 4-5, pp. 217 – 229, 2007.

[11] M. Kim, H. W. Kim, and N. Y. Chong, "Automated robot docking using direction sensing RFID," in *Proc. of IEEE ICRA*, 2007, pp. 4588–4593.

[12] P. Corke, *Robotics, Vision and Control: Fundamental Algorithms in MATLAB*. Springer, 2011.

[13] J. Wang, F. Adib, R. Knepper, D. Katabi, and D. Rus, "RF-compass: Robot object manipulation using RFIDs," in *Proc. of ACM MobiCom*, 2013, pp. 3–14.

[14] D. M. Dobkin, *The RF in RFID: Passive UHF RFID in Practice*. Newton, MA, USA: Newnes, 2007.

[15] "Alien Technology, ALN-9640 Squiggle Inlay," *http://www.alientechnology.com/tags/squiggle/*, 2015.

[16] C. A. Balanis, *Antenna Theory: Analysis and Design, 3rd Edition*. Addison-Wesley Longman Publishing Co., Inc, 2005.

[17] "Alien Technology, ALR-9900+," *http://www.alientechnology.com/products/readers/*, 2016.

[18] "Impinj Inc." *http://www.impinj.com*.

[19] "Directional flat panel antenna PA9-12," *http://www.lairdtech.com/products/pa9-12*, 2016.

[20] S. M. Bowers, A. Safaripour, and A. Hajimiri, "Dynamic polarization control," *IEEE Journal of Solid-State Circuits*, vol. 50, no. 5, pp. 1224–1236, 2015.